2754 Macromolecules 1993, 26, 2754-2758

Remnant Percolative Disorder in Highly-Cured Networks†

Douglas Adolf,*,‡ Brad Hance,‡ and James E. Martin§

Properties of Organic Materials and Advanced Materials Physics Departments, Sandia National Laboratories, Albuquerque, New Mexico 87185

Received November 18, 1992

ABSTRACT: We have previously reported viscoelastic measurements demonstrating that fully-cured networks and critical gels exhibit similar relaxation spectra, implying that fully-cured networks are somewhat ill-connected. Here, we present restricted valence percolation simulations of networks well beyond the percolation transition that explicitly display remnant disorder over length scales less than the correlation length of the network. We conclude that the topology of highly-cured networks is not well described by a regular three-dimensional "tennis net" but is ill-connected over length scales that correspond to relaxation modes of practical interest.

Introduction

The gel point demarks the continuous transition from liquid- to solidlike behavior. The viscoelastic response of critical gels (networks at the gel point) is a peculiar bridge between these disparate states. In fact, it is now well established that the entropic relaxation times for condensation-type critical gels are distributed in the power-law fashion, $H(\tau) \sim \tau^{-\Delta}$.[1-5] Since the sol–gel transition is analogous to a second-order phase transition, this power law should also apply to gels cured somewhat past the gel point for times less than a characteristic time, τ_z. The time, τ_z, which decreases with increasing extent of reaction, corresponds to a length scale ξ, below which the network retains a memory of the structure of the critical gel.

This remnant percolative disorder can be observed in a region of extent of reaction called the *critical regime*.[6] Although the critical regime is expected to be small, we have experimentally shown that the critical regime is actually extremely broad, extending to the fully-cured network for condensation-type cross-linked polymers.[7] For example, we observed distributions of relaxation times in several fully-cured networks given by $H(\tau) \sim \tau^{-\Omega}$ where $\Omega = \Delta$ (see Figure 1), which implies that fully-cured networks have sizable regions of ill-connectedness.

The width of the critical regime can be defined by the manner in which the equilibrium modulus G_∞ increases with extent of reaction α. Scaling arguments predict a simple power-law relationship, $G_\infty \sim \epsilon^z$, where $\epsilon = (p - p_c)/p_c$ and p_c is the bond probability ($p = \alpha^2$) at the gel point. For an epoxy, we observed experimentally that $G_\infty \sim \epsilon^{2.8}$ for all $\alpha > \alpha_c$ (see Figure 2),[8] suggesting a broad critical regime and implying that fully-cured networks contain some degree of remnant percolative disorder. However, because there are no experimental means by which we can directly probe the topology of networks, we were led to computer simulations to investigate the validity of our interpretation of the experimental observations.

Numerous computer simulations have already been performed on networks, so we were at first hesitant to join in the melee. However, the questions we wish to address [(1) *As the network structure evolves, does it exhibit a broad critical regime?* (2) *Does the fully-cured network have some percolative disorder arising from its cure history?*] are not answered in the extant literature. To model fully-cured networks more realistically, we restricted the maximum valence of a node to $b = 3$ although the lattice coordination number is $f = 6$. We use an indirect, dynamical approach—the diffusion of a random walker—to determine the dynamic correlation length of these disordered lattices.

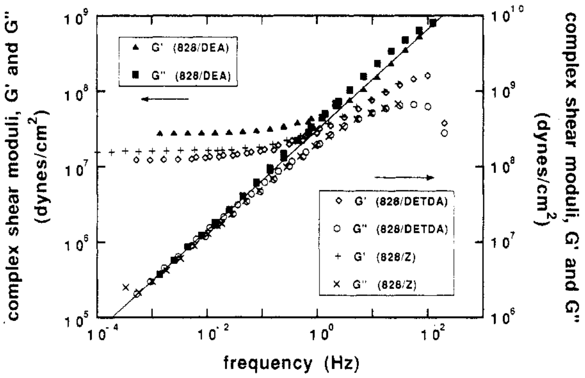

Figure 1. Complex shear moduli for three fully-cured epoxies. The power-law behavior of the loss moduli, $G'' \sim \omega^{2/3}$, mimicks that exhibited by the critical gel.[7]

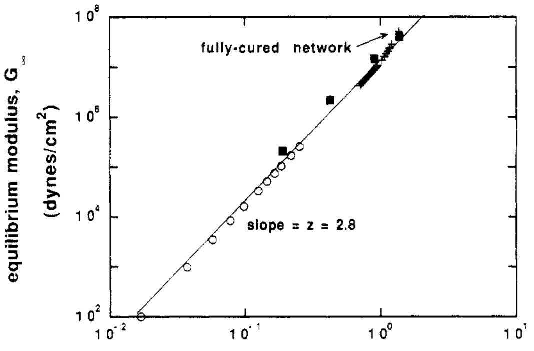

Figure 2. Increase in equilibrium shear modulus, G_∞, with increasing extent of reaction, $\epsilon = |p - p_c|/p_c$. The power-law behavior $G_\infty \sim \epsilon^{2.8}$ is seen over all extents of reaction, even to the fully-cured network, which indicates a wide critical regime.[2]

Approach

Anomalous Diffusion. Some previous percolation simulations[9] have determined the width of the critical regime by taking advantage of the fact that the diffusion on a percolation cluster is anomalous. To understand this approach, we first consider the case of ordinary diffusion on a Euclidean lattice. A random walker on a fully bonded lattice, e.g., a simple cubic lattice, will exhibit the familiar Brownian law $R^2 \sim N$, where R is the root-mean-square excursion distance and N is the number of steps in the

---

† This work was supported by the U.S. Department of Energy under Contract No. DE-AC-04076DP00789.

‡ Properties of Organic Materials Department.

§ Advanced Materials Physics Department.

0024-9297/93/2226-2754$04.00/0

walk. Less familar is the Brownian result $S \sim N^1$ for the number of new sites S visited after N steps. This just says that the probability of a random walker advancing to a new site is a constant that is independent of the number of steps already taken. (Note that S is a purely topological property of the network since it does not depend on how the network is embedded in space.) Both of these standard results are dramatically altered when a random walker is confined to the infinite fractal percolation cluster that occurs at the gel point. Because this cluster contains many dead ends, the random walker finds itself frustrated and is forced to revisit many old sites to make further progress. In fact, the diffusion is so frustrated that the canonical results are invalid, and the anomalous results $R^{3.8} \sim N$ and $S \sim N^{2/3}$ are found. Note that the probability of finding a new site now decreases as $1/N^{1/3}$.

The prescription for network analysis is thus simple: create networks of various extents of reaction; release random walkers on the networks; and determine the dependence of R and S on N. Somewhat beyond the percolation threshold, the walk should be anomalous for small N and Brownian for large N. The crossover N_ξ between the anomalous and Brownian regimes is a measure of the ill-connectedness of the network and can be predicted from scaling arguments. Much beyond the gel point an anomalous regime may not exist. By plotting $S/N^{2/3}$ vs N/N_ξ for networks of increasing extents of reaction beyond the gel point, one can determine the upper limit of the critical regime by identifying the first curve that does not superpose onto the master curve so constructed. We now describe our network model and then consider in greater detail the superposition of diffusion data.

Restricted Valence Percolation. We believe that bond percolation on a simple cubic lattice does not adequately describe the topology of networks at high extents of cure. The fundamental problem is that, although in three dimensions a monomer may have six or more neighbors in contact, it can usually only bond with three or four. Thus a more realistic percolation scheme would allow each node on a lattice of functionality f only b bonds such that $b < f$. This *restricted valence percolation* (RVP)[10] model has been employed for calculating critical exponents, where normal percolation values have been found,[11] but it has not been investigated at high extents of cure. We present RVP results for trivalent nodes on a hexafunctional cubic lattice.

Superposition of Diffusion Data. Before discussing our results, we will consider anomalous diffusion in more detail. For diffusion on the infinite fractal cluster that occurs just at the percolation threshold, it is known that[12]

$$S \sim N^{d_s/2}, \quad N \sim R^{d_w}, \quad S \sim R^{d_f} \qquad (1)$$

where the *spectral dimension* is $d_s \approx {}^4/_3$, the *fractal dimension of the walk* is $d_w \approx {}^{15}/_4$, and the *fractal dimension of the percolation cluster* is $d_f \approx {}^5/_2$. (The spectral dimension is related to the density of vibrational states on a fractal through $g(\omega) \sim \omega^{d_s-1}$.) The fact that S is related to R via the cluster fractal dimension implies that the random walker is so frustrated that as it diffuses it ends up visiting every single site within the radius R. In other words, S/R^{d_f} is of order unity. We also point out that these three relations imply that $d_w = 2d_f/d_s$. In the critical regime, these power laws will also apply past the gel point for walks that span distances less than the correlation length of the network ξ (which diverges as $\xi \sim \epsilon^{-\nu}$ with $\nu \cong 0.89$), since the structure of the network on length scales smaller than ξ is just that of the critical gel.

The observation that the structure of the gel on length scales smaller than the correlation length is just that of the fractal critical cluster allows us to compute how the long-time diffusion constant of a particle diffusing on the gel fraction depends on the extent of cure, or bond probability. We first observe that the time (number of steps) it takes a particle to anomalously diffuse a distance ξ is $T \sim \xi^{d_w}$ (eq 1). Now on longer time and length scales, the diffusion is Brownian (i.e., $S \sim N$ and $R \sim N^{1/2}$) and can be thought of as a random hopping between correlation volumes of size ξ with a hopping time T. Thus the long-time diffusion constant D_∞ is $D_\infty \sim \xi^2/T \sim \xi^{2-d_w} \sim \epsilon^{-\nu(2-d_w)}$ and increases rapidly from zero at the percolation threshold. Finally, we can consider the electrical conductivity of the network, where each bond is assumed to be a resistor of some fixed resistance. An Einstein relation gives the conductivity Σ as the product of the diffusion constant D of a charge carrier times the density ρ of charge carriers. Since only the gel fraction $G \sim \epsilon^\beta$ ($\beta \cong 0.44$) can contribute to the DC conductivity, then $\rho \sim G$ and $\Sigma \sim \epsilon^{\beta+\nu(d_w-2)}$. Defining the conductivity exponent t by $\Sigma \sim \epsilon^t$ ($t \cong 2.0$) gives us the expression $d_w = 2 + (t - \beta)/\nu$ for the walk dimension in terms of standard percolation exponents.

The crossover from anomalous diffusion to Brownian motion at $R = \xi$ can be expressed by the scaling laws[13]

$$S = N^{d_s/2} f_s(N/N_\xi), \quad R = N^{1/d_w} f_R(N/N_\xi) \qquad (2)$$

where $f_s(x) = 1$ for $x \ll 1$, $f_s(x) = x^{1-d_s/2}$ for $x \gg 1$; and $f_R(x) = 1$ for $x \ll 1$, $f_R(x) = x^{1/2-1/d_w}$ for $x \gg 1$. The crossover N_ξ is the number of steps required to travel a distance ξ and, in the critical regime, scales as

$$N_\xi \sim \xi^{d_w} \sim S_\xi^{\,2/d_s} \sim \xi^{2d_f/d_s} \sim \epsilon^{-2d_f\nu/d_s} \qquad (3)$$

Therefore, plots of $S/N^{d_s/2}$ or $R/N^{1/d_w}$ versus N/N_ξ at various extents of reaction will superpose in the critical regime. Only data that superpose are within the critical regime, and this process allows us to unambiguously determine the domain of remnant percolative disorder.

Network Topology. To determine the dynamic correlation length, we used the following procedure. We define the apparent diffusion coefficient as $D_{app}(N) \sim R^2/N$. As shown above, the apparent diffusion coefficient approaches the constant, $D_\infty \sim \xi^2/N_\xi \sim \xi^{2-d_w}$, in the limit of long walks ($N \gg N_\xi$). For short walks ($N \ll N_\xi$), the apparent diffusion coefficient will scale as $D_{app} \sim N^{2/d_w-1}$. Stated equivalently, the apparent diffusion coefficient has the scaling form $D_{app} = D_\infty f(N/N_\xi)$ where $f(x) = x^{-(1-2/d_w)}$ for $x < 1$ and $f(x) = 1$ for $x > 1$. Taking prefactors to be of order unity, a suitable expression for $f(x)$ for all x is $f(x) = 1 + x^{-(1-2/d_w)}$. Therefore, the apparent dynamic correlation length is given by

$$\xi_{app}(N) = [D_{app} - N^{-(1-2/d_w)}]^{1/(2-d_w)} \qquad (4)$$

which should be a constant, ξ, for all N.

A simple static analysis of our simulation networks yields the gel fraction and the distribution of mono-, di-, and trifunctional nodes (n_1, n_2, n_3) in the gel fraction. The fraction of monofunctional nodes can be interpreted as the fraction of "dangling chains" in the gel; the fraction of difunctional nodes can be related to the average chain length between cross-links; and the fraction of trifunctional nodes gives the cross-link density, which, in the simplest theories of network elasticity, is proportional to the number of "elastically effective chains" and thus the equilibrium modulus.[14]

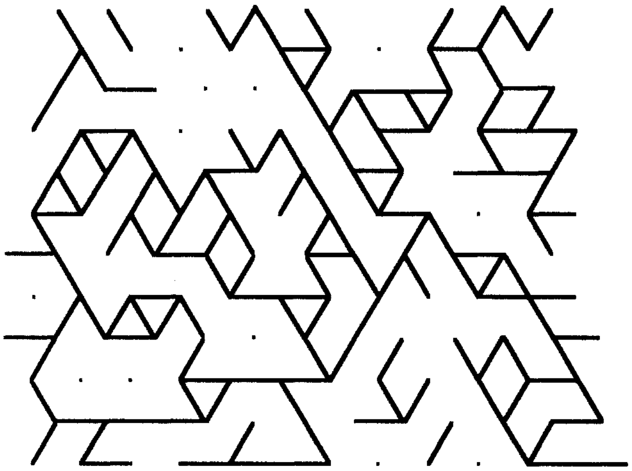

Figure 3. Example of the ill-connectedness of restricted valence percolation networks even at high extents of reaction. The network shown is two-dimensional at $p = 0.85$ ($p_c = 0.6$).

Simulation Technique

Network Generation. Networks of various bond probabilities were generated on a simple cubic lattice (40 × 40 × 40) with cyclic boundary conditions by creating a list of potential bonds (those for which vicinal nodes are not yet trivalently bonded) and randomly choosing one bond to fill. That bond is then removed from the list and the process continued until the desired extent of bonding is attained. Fully bonded networks cannot be created because random bonding leaves divalent nodes without any bondable neighbors, and other defect structures. Such inherent RVP defects are not found in lattices where $b = f$. We cannot conveniently convey the ramified structure of our three-dimensional networks, but, in Figure 3, a two-dimensional network with $p = 0.85$ ($p_c = 0.6$) is shown that exhibits similar ill-connectedness.

Cluster Distribution. For each network, we calculated the distribution of cluster sizes by first identifying each cluster using a method of cluster "coloring". First each node j is given the color "j". Then, each node is examined in sequence and recolored with the lowest color of any of its bonded neighbors. After a finite number of iterations, the process converges so that all the nodes of each connected cluster are the same unique color. Then one simply counts the number of nodes of each remaining color to obtain the cluster size distribution. To determine if a spanning cluster exists (i.e., that the network has "gelled"), we recolored the clusters after eliminating the cyclic boundary conditions and evaluated whether the largest cluster has nodes at opposite boundaries. The gel point was taken as the bond probability at which the largest cluster spans the lattice. Since this is a finite system, the critical bond probability, p_c, which was found to be 0.4945 ± 0.0002, is somewhat smaller than that of the infinite lattice. (For a simple cubic lattice of the same size, we found $p_c = 0.2433 \pm 0.0002$, whereas $p_c = 0.247$ for the infinite lattice.[15]) Note that the product of $bp_c = 3(0.4945) = 1.484$ for our RVP simulations agrees well with the normal bond percolation quasi-invariant $bp_c = 1.5$,[15] even though a functionality of 3 is impossible to simulate by normal bond percolation in three dimensions.

Random Walks. At a given extent of reaction (bond probability) past the gel point, we then took 200 random walks of 100 000 steps each on the largest cluster (the gel fraction). For each walk, we calculated the distance R from the walk origin and the number of new sites S visited as a function of step number N. The calculation of S required us to keep tract of whether or not we had visited a site before; if cyclic boundary conditions were not in force, we could merely initialize each node with the value 1 and reduce this to 0 after we visited the site while simultaneously increasing S by 1 (analogous to picking up bread crumbs as we go). However, the cyclic boundary conditions require us to also keep track of how we get to a node. To understand how this was accomplished, suppose we are walking on a one-dimensional lattice with cyclic boundary conditions, and each node has a 3-bit integer value associated with it and initialized to binary 111. If we are walking on the original lattice and visit the jth site for the first time, we set the integer to binary 101 and increment S. If we step onto the image lattice to the left and visit the jth site again, we set the node value to 001 and increment S, and if we step onto the image lattice to the right and visit the jth site again, we set the node value to 000 and increment S. We do not attempt to keep track of more distant image lattices. To accomplish this in three dimensions, we considered a 3 × 3 × 3 cube of 27 lattices by using 27 of the bits of a 32-bit integer. We could thus allow the walk, which starts in the central cube, to travel into neighboring lattices, thereby effectively increasing the size of our 40 × 40 × 40 lattice to 120 × 120 × 120 (technically, this approach is strictly valid only when the true correlation length is shorter than the fundamental lattice size). The distance and site calculations were then averaged over all walks. All codes were written in "C" and ran in less than 6 h on a Macintosh SE/30.

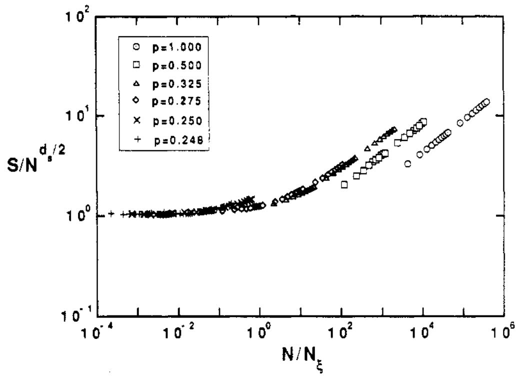

Figure 4. Master plot of new sites visited S per steps walked N for random walks on simple cubic lattice percolation networks at various extents of reaction past the gel point. Superposition is seen only for networks with $p < 0.325$ ($p_c = 0.2433$).

Results

Simple Cubic Lattice. In order to obtain base-line data that we can compare to the restricted valence percolation model, we first obtained results for the simple cubic lattice (SCL) with $b = f = 6$. Figures 4 and 5 show the scaled plots of the number of new sites S visited and walk distance R as functions of N for networks of increasing bond probabilities. On short length scales, $N < N_\xi$, the master curves have zero slope, indicating anomalous diffusion, which crosses over to the much more rapid Brownian diffusion for $N > N_\xi$. For the hexafunctional cubic lattice, the critical bond probability is 0.2433 ± 0.0002, and since the curves certainly do not superpose for $p \geq 0.325$, the critical regime extends to $\epsilon \simeq 0.3$. Figure 6 shows the apparent dynamic correlation length from eq 4 for networks of differing extents of reaction. The correlation length for the completely bonded network equals 1.1.

Restricted Valence Percolation. In Figures 7 and 8, we present the scaled plots of the number of new sites S visited and walk distance R as functions of N for networks

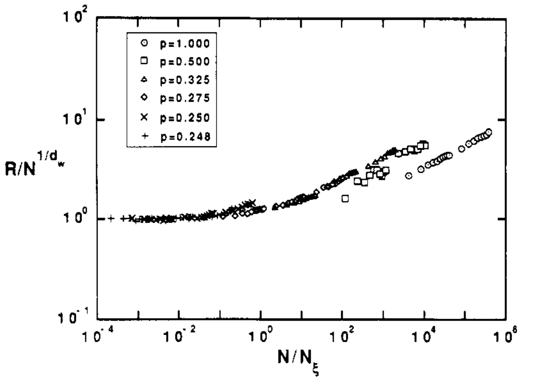

Figure 5. Master plot of distance traveled R per steps walked N for random walks on simple cubic lattice percolation networks at various extents of reaction past the gel point. Superposition is seen only for networks with $p < 0.325$ ($p_c = 0.2433$).

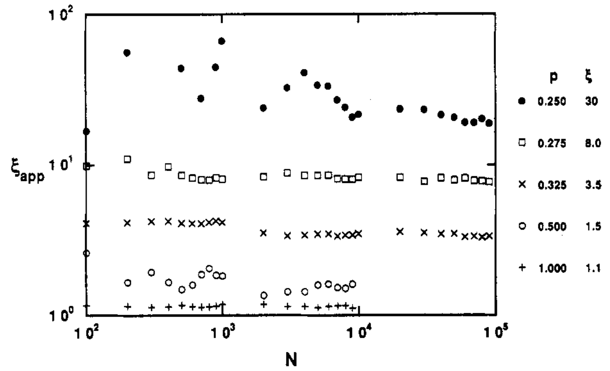

Figure 6. Apparent correlation length defined in eq 4 for simple cubic lattice percolation networks at various extents of reaction past the gel point. Values for the correlation length as a function of ϵ are tabulated at the right of the figure.

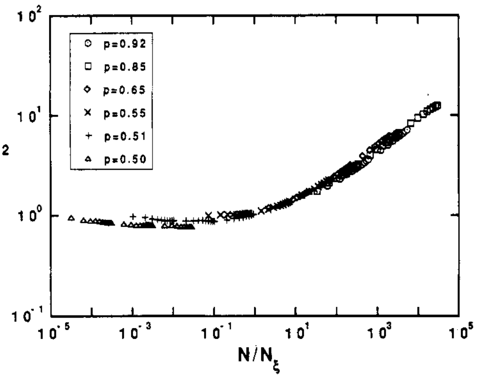

Figure 7. Master plot of new sites visited S per steps walked N for random walks on RVP networks at various extents of reaction past the gel point. Superposition is seen only for networks with $p < 0.65$ ($p_c = 0.4945$).

generated by the restricted valence percolation scheme. Again, we see anomalous diffusion that crosses over to Brownian diffusion at N_ξ. The critical bond probability is 0.4945 ± 0.0002 for this RVP simulation in which $b = 3$ and $f = 6$. The curves superpose to $p = 0.65$ indicating that the critical regime extends to $\epsilon \cong 0.3$. Figure 9, again, shows the apparent dynamic correlation length from eq 4 for networks of differing extents of reaction. The correlation length for the completely bonded network equals 2.0.

Discussion

We first will answer the two questions posed in the introduction: (1) *As the network structure evolves, does it exhibit a broad critical regime?* (2) *Does the fully-cured network have some percolative disorder arising from its cure history?* Our simulations do indicate a broad critical regime extending to at least $\epsilon \cong 0.3$ as judged by superposition of walk data. Moreover, walk data from fully-bonded RVP networks do not show dramatic deviations from superposition, supporting the experimental results in Figure 2 that suggest a critical regime which extends to the fully-cured network. As to the question of remnant percolative disorder, even though fully-bonded SCL networks exhibit no disorder, fully-bonded RVP networks do exhibit ill-connectedness, as evidenced by $\xi \cong 2$.

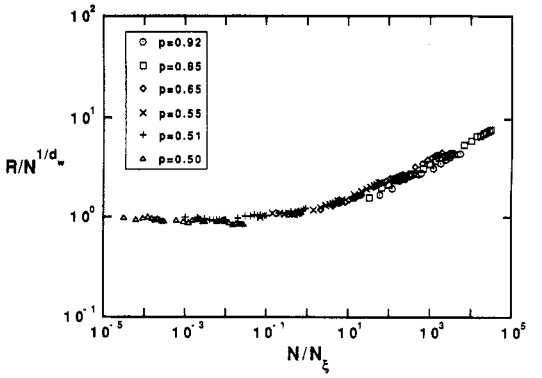

Figure 8. Master plot of distance traveled R per steps walked N for random walks on RVP networks at various extents of reaction past the gel point. Superposition is seen only for networks with $p < 0.65$ ($p_c = 0.4945$).

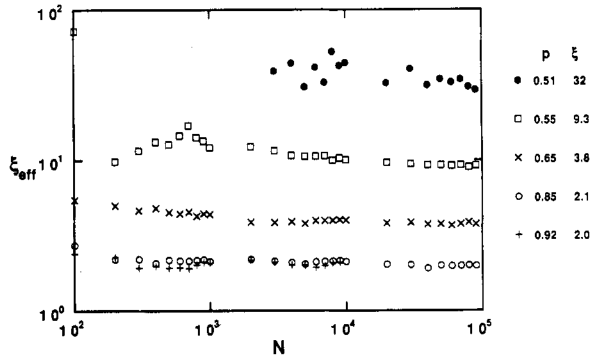

Figure 9. Apparent correlation length defined in eq 4 for RVP networks at various extents of reaction past the gel point. Values for the correlation length as a function of ϵ are tabulated at the right of the figure.

The concept of remnant percolative disorder warrants a more detailed discussion. At the percolation transition, fractal clusters exist on all size scales, so that the ensemble is self-similar on length scales from somewhat larger than the monomer size, a, to infinity. As the reaction progresses, the correlation length, ξ, which is the upper length over which either the gel fraction or the sol fraction is self-similar, decreases. At length scales larger than ξ, the network appears as a Euclidean lattice. Since the simulation results indicate that the correlation length of the fully-cured RVP network is greater than the monomer size, even fully-cured networks have microdomains of remnant percolative disorder. Thus the viscoelastic response of the fully-cured network on time scales that are short compared to the normal modes of units of size ξ will be similar to the dynamics of the critical gel, as seen experimentally.

It may seem that such limited topological disorder ($\xi = 2$) cannot give rise to the 3–4 decades of power-law viscoelastic relaxation observed for fully-cured epoxy networks (Figure 1). However, our previous studies revealed that relaxation times in condensation-type net-

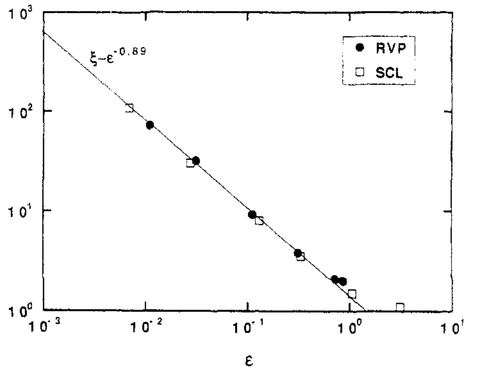

Figure 10. Correlation length for SCL and RVP networks at various extents of reaction past the gel point. The data form a master curve which should be valid for all normal bond and restricted valence percolation simulations regardless of lattice or node functionality.

works scale with size[1] as $\tau \sim R^{4.5}$, so relatively small regions of topological disorder can result in many decades of power-law decay. Moreover, it seems reasonable that the correlation length calculated from our simulations is a lower bound for real polymers, which usually have unequal reactivities and/or bond correlations.

At low frequencies corresponding to length scales larger than the correlation length, viscoelastic measurements may deviate from the critical gel power-law relaxation, if it were possible to determine the loss modulus for such elastic materials for which $\tan \delta = G''/G' < 0.01$. However, from a practical view such as vibration damping, only those relaxations for which $\tan \delta > 0.1$ are important. Therefore, the power-law relaxation mechanism is, in practice, the only entropic relaxation mechanism of interest, implying that the microdomains of percolative disorder determine the relavent viscoelastic behavior of fully-cured networks.

We now examine how the degree of percolative disorder depends on extent of reaction. Figure 10 shows the dependence of ξ on ϵ for both RVP and SCL networks. For $\epsilon \leq 0.3$, $\xi \sim \epsilon^{-0.89}$, the appropriate percolation scaling law near the gel point. The departure from this scaling law at $\epsilon = 0.3$ explains why superposition of walk data fails for $\epsilon > 0.3$ and also defines the width of the critical regime. The data in Figure 10 for both RVP and SCL networks generate a master curve, which should be valid for all normal bond and restricted valence percolation simulations regardless of lattice or node functionality. Therefore, the procedure for determining the correlation length at a given bond probability is straightforward: determine the gel point, $p_c = 1.5/b$, where b is the node functionality of the percolation scheme of interest ($b = f$ for normal bond percolation); calculate $\epsilon = p/p_c - 1$ at the given bond probability; and find $\xi(\epsilon)$ from the master curve of Figure 10. Unusual percolation schemes, such as those where reaction probabilities depend on a node's current functionality, will be exceptions to the rule.

Figure 11 shows the gel fraction and the n_1, n_2, n_3 nodes of the spanning cluster. The gel fraction follows the percolation power-law prediction of $\epsilon^{0.44}$ for $\epsilon < 0.3$ in agreement with our previous observations. The quantity n_3 is proportional to the number of effective chains and the equilibrium modulus G_∞ in the simplest theories of rubber elasticity. In Figure 2, our experimental results for the increase in G_∞ with extent of reaction indicate $G_\infty \sim \epsilon^{2.8}$, in good agreement with our previous theoretical prediction[1] of $G_\infty \sim \epsilon^{2.7}$ but vastly different from the behavior of n_3 in Figure 11. This discrepancy indicates that the simple theories of rubber elasticity do not correctly predict the increase in the number of effective chains with the extent of reaction.

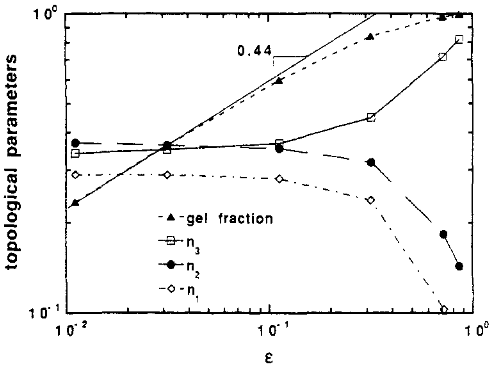

Figure 11. Gel fraction and 1-, 2-, and 3-functional nodes of the spanning cluster for RVP networks at various extents of reaction.

Conclusions

Restricted valence percolation simulations of networks at various extents of reaction indicate a wide critical regime and microdomains of percolative disorder in fully-bonded networks. These results agree with our previous viscoelastic measurements which demonstrate that fully-cured networks exhibit relaxation spectra similar to the spectra of critical gels. Therefore, the topology of fully-cured networks is not a regular three-dimensional "tennis net" but exhibits ill-connectedness over length scales corresponding to relaxation modes of practical interest.

References and Notes

(1) Martin, J. E.; Adolf, D.; Wilcoxon, J. P. *Phys. Rev. A* **1989**, *39*, 1325.
(2) Adolf, D.; Martin, J. E.; Wilcoxon, J. P. *Macromolecules* **1990**, *23*, 527.
(3) Chambon, F.; Winter, H. H. *J. Rheol.* **1987**, *31*, 683.
(4) Durand, D.; Delsanti, M.; Adam, M.; Luck, J. M. *Europhys. Lett.* **1987**, *3*, 297.
(5) Rubinstein, M.; Colby, R. H.; Gillmor, J. R. In *Space-Time Organization in Macromolecular Fluids*; Tanaka, F., Doi, M., Eds.; Springer-Verlag: Berlin, 1989.
(6) Stauffer, D.; Coniglio, A.; Adam, M. *Adv. Polym. Sci.* **1982**, *44*, 103.
(7) Adolf, D.; Martin, J. E. *Macromolecules* **1991**, *24*, 6721.
(8) Adolf, D.; Martin, J. E. *Macromolecules* **1990**, *23*, 3700.
(9) Argyrakis, P.; Kopelman, R. *J. Chem. Phys.* **1985**, *83*, 3099.
(10) Gaunt, D. S.; Guttmann, A. J.; Whittington, S. G. *J. Phys. A* **1979**, *12*, 75.
(11) Kertesz, J.; Chakrabarti, B. K.; Duarte, J. A. M. S. *J. Phys. A* **1982**, *15*, L13.
(12) Alexander, S.; Orbach, R. *J. Phys. (Paris)* **1982**, *43*, L625.
(13) Havlin, S.; Ben-Avraham, D.; Sompolinksy, H. *Phys. Rev. A* **1983**, *27*, 1730.
(14) Flory, P. J. *Principles of Polymer Chemistry*; Cornell University Press: Ithaca, NY, 1953.
(15) Zallen, R. *The Physics of Amorphous Solids*; Wiley: New York, 1983.